

# Multi-objective Optimization of A-Class Catamaran Foils Adopting a Geometric Parameterization Based on RBF Mesh Morphing

Marco Evangelos Biancolini<sup>1</sup>, Ubaldo Cella<sup>1,2\*</sup>, Alberto Clarich<sup>3</sup> and Francesco Franchini<sup>4</sup>

<sup>1</sup> University of Rome “Tor Vergata”, Roma, Italy

<sup>2</sup> Design Methods (www.designmethods.aero), Messina, Italy

<sup>3</sup> ESTECO (www.esteco.com), Trieste, Italy

<sup>4</sup> EnginSoft (www.enginsoft.com), Firenze, Italy

\* Corresponding author. E-mail address: ubaldo.cella@designmethods.aero

**Abstract** The design of sailing boats appendages requires taking in consideration a large amount of design variables and diverse sailing conditions. The operative conditions of dagger boards depend on the equilibrium of the forces and moments acting on the system. This equilibrium has to be considered when designing modern fast foiling catamarans, where the appendages accomplish both the tasks of lifting up the boat and to make possible the upwind sailing by balancing the sail side force. In this scenario, the foil performing in all conditions has to be defined as a trade-off among contrasting needs. The multi-objective optimization, combined with experienced aerodynamic design, is the most efficient strategy to face these design challenges. The development of an optimization environment has been considered in this work to design the foils for an *A-Class* catamaran. This study, in particular, focuses on the geometric parameterization strategy combined with a mesh morphing method based on Radial Basis Functions, and managed through the workflow integration within the optimization environment.

**Keywords:** multi-objective optimization, mesh morphing, Radial Basis Functions, foiling catamarans, aerodynamic design.

## 1 Introduction

“*Foiling*” (term used to describe a sailing condition in which the boat is lifted up from the water by lifting surfaces) is not a new idea in the sailing world (the first known sailing hydrofoil was produced in 1938 by Robert Rowe Gilruth and

Carl William Price [1]) but, as it often occurred for many innovative solutions, the efficient exploitation of its potentialities was related to the technological improvements in materials, manufacturing processes, design capability, etc. The foiling solutions adopted in the last America's Cup class catamarans (called AC72) gave a strong impulse to the evolution of smaller multihull classes. The A-Class catamaran has benefited from these experiences and have shown significant innovations in the last few years due to its large diffusion and open rules.

The A-Class, born in the late 50s, is a small high-tech catamaran that is considered the fastest single-handed racing dingy in the world. The rules are very simple. They mainly constrain the minimum weight (75 Kg), the hulls length (18 ft) and the sail surface (150 ft<sup>2</sup>). In 2009 new rules were added with the intention of preventing foiling for A-Cats. Given that the concept of *hydrofoiling prohibition* was ambiguous and difficult to define, an indirect approach was chosen. The idea was to introduce a set of constraints aimed to limit the surfaces suitable for sustaining the boat so to return unfavourable a flying configuration compared to a traditional one. The constraints were defined assuming a reference vertical force coefficient that, in absence of previous experience, was evaluated from the operative conditions of the Moth class foils (the estimated lift coefficient was 0.4). Such assumption showed to be conservative and allowed the development of very favourable flying configurations. The rules, therefore, make the foil dimensioning a strongly constrained design problem for which efficient implementation of multi-objective optimizations might represent the key strategy to design configurations able to broaden the range of sailing conditions in which flying boats are faster than conventional ones.

Novel solutions were traditionally tested, in A-Cats, with empirical *trial and error* approach. The improvement and the availability of engineering numerical tools (CFD, FEM, MDO...), combined to the increase of the computational resources power, contribute today to reduce the costs of advanced engineering methodologies (which in the recent past were limited to research contests or to high technological fields as the aerospace). Highly specialized engineering services are then now beginning to be compatible with the requirements of relatively limited markets as the sports dinghies. For this reason, a joint project including the university of Rome "*Tor Vergata*", the aerospace engineering consulting firm *Design Methods* and the software vendors *RBF Morph*<sup>1</sup> and *ESTECO*, has been developed to setup a pilot study to demonstrate capabilities and the potentialities of combining cutting edge mesh morphing technologies and optimization design environments by developing a highly constrained multi-objective optimization procedure.

The implementation of strongly constrained geometric parameterization often suggests adopting a parametric CAD system coupled to a numerical domain regeneration procedure. In this paper, we want to demonstrate the efficiency of the mesh morphing approach based on Radial Basis Functions (using *RBF Morph*).

---

<sup>1</sup> [www.rbf-morph.com](http://www.rbf-morph.com)

The optimization procedure consists in combining two-phases CFD simulations of the foils, using the *ANSYS Fluent* solver, with the mesh morphing tool *RBF Morph* within the *ESTECO modeFRONTIER* optimization workflow. The design variables control the foil planform and the front shape subjected to geometrical constraints. The objective functions are defined to improve the performances in upwind (navigation against the wind) and downwind (navigation with the wind) sailing conditions at two values of boat speed.

## 2 Shape parameterization by mesh morphing

The geometric parametrization based on mesh morphing consists in implementing shape modifiers, amplified by parameters that constitute the problem variables, directly on the computational domain. New geometric configurations are obtained imposing the displacement of a set of mesh regions (e.g. walls, boundaries or discrete points within the volume) by using algorithms able to smoothly propagate the prescribed displacement to the surrounding volume. The performances of the morphing action (in terms of quality of the morphed mesh and computational resources requirements) depend on the algorithm adopted to perform the smoothing of the grid. Among the several algorithms available in literature, Radial Basis Functions are recognized to be one of the best mathematical framework to deal with the mesh morphing problem [2].

The first commercial mesh morphing software based on Radial Basis Functions was *RBF Morph*. The tool was born as an add-on of the *ANSYS Fluent* CFD code, fully integrated in the solving process, and was launched to the market in 2009 [3]. Its efficiency was successfully demonstrated on several industrial engineering problems (shape optimization, ice accretion, static and dynamic FSI analyses) [4] including application with sails [5] and structural problems [6]. Today *RBF Morph* is also suitable as a stand-alone tool to be coupled with any solver.

Several advantages are related to the RBF mesh morphing approach:

- there is no need to regenerate the grid;
- the robustness of the procedure is preserved;
- its meshless nature allows to support any kind of mesh typology;
- the smoothing process can be highly parallelizable;
- the morphing action can be integrated in any solver.

The latter feature offers the very valuable capability to update the computational domain “on the fly” during the progress of the computation.

The main disadvantages of RBF mesh morphing methods are the requirement of a “back to CAD” procedure, some limitation in the model displacement amplitude, due to the distortion occurring after extreme morphing, and the high computational cost related to the solution of the RBF system that, if large computational domains are involved, imposes the implementation on HPC environments.

## 2.1 Radial Basis Functions

Radial Basis Functions (RBF) are powerful mathematical functions able to interpolate, giving the exact values in the original points, functions defined at discrete points only (source points). The interpolation quality and its behaviour depends on the chosen RBFs. A linear system (of order equal to the number of source points introduced) needs to be solved for coefficients calculation. Once the unknown coefficients are calculated, the motion of an arbitrary point inside or outside the domain is expressed as the summation of the radial contribution of each source point (if the point falls inside the influence domain). An interpolation function composed by a radial basis and a polynomial is defined as follows:

$$s(x) = \sum_{i=1}^N \gamma_i \phi(\|x - x_i\|) + h(x) \quad (1)$$

The minimal degree of polynomial  $h$  depends on the choice of the basis function. A unique interpolant exists if the basis function is a conditionally positive definite function. If the basis functions are conditionally positive definite of order  $m = 2$ , a linear polynomial can be used:

$$h(x) = \eta + \eta_1 x + \eta_2 y + \eta_3 z \quad (2)$$

The values for the coefficients  $\gamma$  of RBF and the coefficients  $\eta$  of the linear polynomial can be obtained by solving the system

$$\begin{pmatrix} M & P \\ P^T & 0 \end{pmatrix} \begin{pmatrix} \gamma \\ \eta \end{pmatrix} = \begin{pmatrix} g \\ 0 \end{pmatrix} \quad (3)$$

where  $g$  are the known values at the source points.  $M$  is the interpolation matrix defined calculating all the radial interactions between source points

$$M_{ij} = \phi(\|x_{k_i} - x_{k_j}\|) \quad 1 \leq i \quad j \leq N \quad (4)$$

and  $P$  is the constraint matrix

$$P = \begin{pmatrix} 1 & x_{k_1}^0 & y_{k_1}^0 & z_{k_1}^0 \\ 1 & x_{k_2}^0 & y_{k_2}^0 & z_{k_2}^0 \\ \vdots & \vdots & \vdots & \vdots \\ 1 & x_{k_N}^0 & y_{k_N}^0 & z_{k_N}^0 \end{pmatrix} \quad (5)$$

The radial basis is a meshless method suitable for parallel implementation. In fact, once the solution is known and shared in the memory of each node of the cluster, each partition has the ability to smooth its nodes without taking care of

what happens outside because the smoother is a global point function and the continuity at interfaces is implicitly guaranteed.

## 2.2 RBF Morph setup

*RBF Morph* allows to extract and control points from surfaces and edges, to put points on primitive shapes (boxes, spheres and cylinders) or to specify them directly by individual coordinates and displacements. Primitive shapes can be combined in a Boolean fashion limiting the action of the morpher itself. The shape information coming from an individual RBF setup are generated interactively with the help of the GUI and are used subsequently in batch commands that allow to combine many shape modifications in a non-linear fashion (non-linearity occurs when rotation axis are present in the RBF setup). The displacement of the prescribed set of source points can be amplified according to parameters that constitutes the parametric space of the model shape.

The definition and the execution of a morphing action is completed by the following steps: *setup*, *fitting* and *smoothing*. The setup consists in the manual definition, from the program GUI, of the domain boundaries within which the morphing action is limited to, in the selection of the source points where fixed and moving mesh regions are imposed, and in the definition of the required movements of the points used to drive the shape deformation. During the fitting process, the RBF system, derived from the problem setup, is solved and stored into a file ready to be amplified. This operation has to be performed only once for every RBF problem. Stored RBF solutions are very light (in terms of files dimension) compared to storing all the created morphed mesh. The smoothing action (surfaces and volumes morphing according to arbitrary amplification factors) is first performed applying the prescribed displacement to the grid surfaces and then smoothly propagating the deformation to the surrounding domain volume. It can be performed combining several RBF solutions, each one defined by a proper amplification factor, to constitute the parametric configuration of the computational domain. Figure 1 reports an example (in this case applied to the sail) of and RBF problem setup.

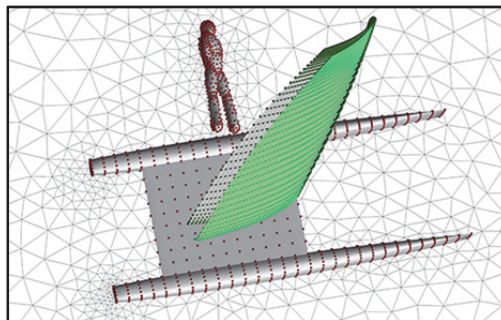


Figure 1: Fixed (red) and moving (green) source points of an RBF setup.

### 3 Foils design problem description

The operative conditions of sailing boats appendages depend on the equilibrium of the forces and moments acting on the system [7]. The speed is related to the performances of sails and to the characteristics of the boat with a complex interaction whose estimation require to model the several aspects of the physics involved. For this reason the design of any components should be, in general, approached within so-called VPP (Velocity Prediction Program) environments [8].

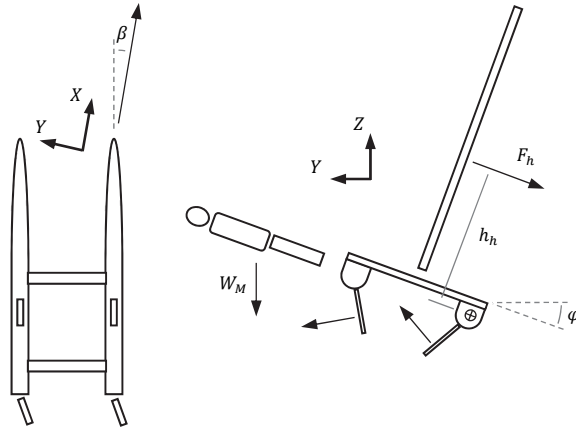


Figure 2: Forces acting on the boat.

To define the design conditions of the A-Cat foils, some simplifications has been, however, adopted in this work. The vertical force equilibrium is mainly dominated by the weight of the boat and the crew. The modulus of the other components, derived from the 6DoF equilibrium, varies in a range that is, in general, smaller than the range of possible crew weight. It is then considered acceptable for the foils to assume a fixed target vertical component of the lift. Similar assumptions are accepted for the side force since it is mainly limited by the maximum righting moment generated by the helmsman at the trapeze (for a fixed known height of the sail centre of effort  $h_h$ ). The task is to identify the shape of the foils that, while respecting the imposed constraints and generating the required lifting force components, minimize the drag [9].

#### 3.1 Geometric constraints definition

A-Class rules state that all foils have to be inserted from the top of the hull (to prevent the adoption of *T-foils*) and that the minimum distance between the tips must always be larger than 1.5 m (to limit the span of surfaces contributing to the vertical lift). The maximum beam of the boat, including appendages in all positions, must be lower than 2.3 m. In order to insert the foils, furthermore, a mini-

imum value of the angle  $\delta$ , assuming *L-shaped* foils, is required (Figure 3). Finally, structural requirements impose a minimum value of the foil thickness.

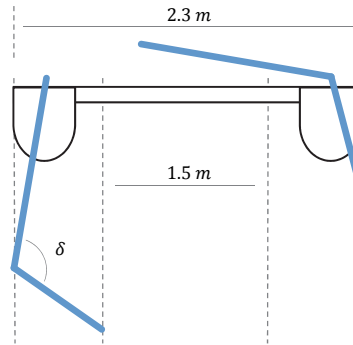


Figure 3: Scheme of foils constraints.

## 4 Setup of numerical model

A two-objective optimization procedure was setup within the *modeFRONTIER* software environment. The objectives are defined by the minimization of the boat hydrodynamic drag, excluding the rudders, in upwind and downwind sailing conditions. In downwind sailing the boat is expected to be fully lifted up from the water by the foils. Configurations that are not able to generate sufficient lift are rejected. In upwind sailing, the boat is expected to be only partially sustained by the foils.

### 4.1 CFD configuration

A steady incompressible analysis, using a volume of fluid (VOF) technique to model the two-phases (air and water), was setup for the downwind analysis. The boat was assumed to sail at a heeling angle (angle  $\varphi$  of Figure 2) of five degree and at a speed of 15 knots. The sinkage was iteratively trimmed to define the attitude that generates the target vertical force. No cavitation model was activated<sup>2</sup>. The total displacement was assumed equal to 170 Kg (empty boat weight plus crew). Considering around 30% of this value to be generated by the *T-foils* of the two rudders, the main foils were then assumed to contribute with the generation of 120 Kg to the sustainment of the boat. The operative leeway angle (angle  $\beta$  of Figure 2) should be defined from the global equilibrium of forces and moments acting on the boat. In was, however, here considered acceptable to keep it fixed to

<sup>2</sup> The cavitation critical  $C_p$ , at the selected downwind speed, is around -3 [10]. Such value is not expected to be reached in the design conditions (especially if laminar airfoils are adopted).

3 deg. The proper estimation of its value would have, in fact, significantly increased the computational burden since it requires to introduce an additional degree of freedom. The balance between the additional computational cost required and the impact this simplification is expected to have on the optimization trend fully justifies, in our view, this choice.

The analysis in upwind sailing was performed at a speed of 10 knots and at a fixed attitude maintaining the computational domain unchanged (also in this case it was assumed five degree as heeling angle). One hull is flying while the other one is floating and contributing to the sustainment. A single phase CFD analysis was setup assuming the top inviscid wall boundary of the domain (which, in order to partially account for hull/foil junction interference effects, includes a shape similar to the immersed hull) to represent the water free surface considered as planar (Figure 4). This simplification force to neglect effects as ventilation or hull boundary layer interference introducing uncertainties on the solution. It is, however, considered acceptable, for the optimization purpose, since the aim to estimate the drag difference between candidate solutions is prevalent on the necessity of an accurate definition of the absolute value of drag. The missing drag component of the hull is recovered by an analytical formulation developed by a comparison with a matrix of CFD solutions obtained on the isolated demihull at several attitudes and displacements (a description of the formulation adopted is reported in [11]). The lift fraction obtained subtracting the lift generated by the foils from the boat operative displacement is used to feed the hull analytical drag model, whose output is added to the foils drag fraction to generate the objective function.

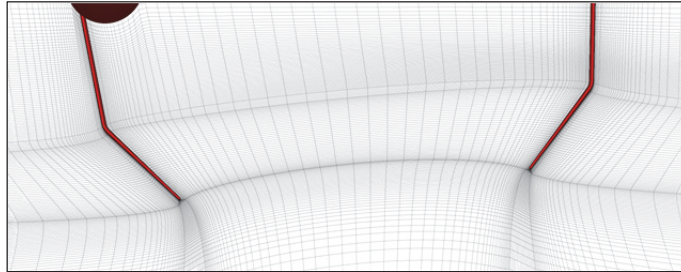


**Figure 4: Detail of the computational domain (medium mesh)**

The accurate evaluation of the leeway angle is considered to be important in upwind sailing and adjusted by changing the inflow direction on the far field boundaries. Its operative value is estimated performing two preliminary analyses at two angles and then linearly extrapolating the final leeway angle at which the candidate geometry generates the required target side force. If the target side force is not generated at the expected angle, the selected configuration is rejected because it does not perform in the linear region of the aerodynamic lift polar. The target side force (in our case defined equal to 70 Kg) was estimated from the equilibrium of moments around the sailing direction assuming a value for the height of the sailing centre of effort (distance  $h_h$  of Figure 2) of 4 meters.

### Computational domain

A multi-block structured hexahedral mesh was generated modelling a domain extended up to ten meters upstream and downstream the foils. It is ten meters wide and five meters deep. The top of the domain coincides with the water level in up-wind conditions. Three levels of grid were generated (Figure 5) with the aim to evaluate the sensitivity of the solution on the grid dimension. The size of coarse, medium and fine meshes were approximatively 1, 7.5 and 25 millions of cells.

Figure 6 reports the solutions obtained, on the baseline geometry, with the three meshes in downwind configuration (VOF analysis trimming the sinkage to maintain the vertical lift component unchanged). The difference between the drag obtained with the coarse grid and the drag obtained adopting the fine mesh is in the order of 5% while the adoption the medium grid led to a difference limited to half percent. The coarse mesh was the one used in the optimization procedure.



Figure 5: Surface cells clustering for the three levels of grid.

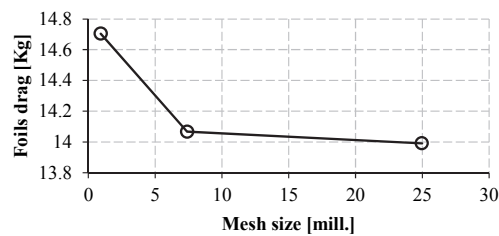


Figure 6: Solution sensitivity to the grid dimension.

### 4.2 Implementation of shape parameterization

The reference geometry is made by two straight segments smoothly blended in the junction region. The connection with the hulls is located at the external side and both inner and outer segments are oriented inboard. This configuration is assumed to offer flying stability advantages (which are not accounted by the optimization criterion) with respect to an inner segment bent outboard (as the sketch in Figure 3) [12]. The location of the hull/foils junction is then not a design variable.

The foils segments are generated by a straight untwisted extrusion of the well-known NACA 63-412 laminar airfoil<sup>3</sup>. The inner section is assumed to have a constant chord while the outer is tapered.

The variables of design were:

1. total foil draft;
2. outer segment cant angle (angle  $\delta$  of Figure 3);
3. angle of the inner segment respect to vertical;
4. inner segment chord (keeping the absolute foil thickness unchanged);
5. outer segment taper ratio;
6. foils sweep angle.

The last parameter is not exactly a shape parameters. It is a trim that has a direct effect on the horizontal angle of incidence of the foils. Its morphing action is implemented as a rotation of the foils along an axis perpendicular to the boat symmetry plane and passing near the hull/foil junction.

Seven shape modifiers have been setup: four to control lengths and angles of the foil segments (Figure 7), one to set the chord of the inner segment, one for the taper ratio of the outer segment and one to control the foils sweep angle. The amplification factors of the RBF solutions are defined combining the design input variables in order to fulfil the constraints imposed by the class rules (e. g. when the cant angle  $\delta$  is modified, the outer segment is scaled according to an amplification factor that recover the limits reported in Figure 3). The morphing actions are applied in sequence and limited to a volume surrounding the foils region.



**Figure 7: Foils front shape modifiers**

### ***4.3 Integration in the optimization environment***

The multi-objective design software *modeFRONTIER* allows to integrate different computational codes (any commercial or in-house tools) into a common design environment. It allows the automatic execution of a series of designs pro-

---

<sup>3</sup> The airfoil design is not included in this phase. The foils are analyzed by fully turbulent RANS analyses with the view to demand the verification of the laminar stability and the proper operating range of the airfoil to a following design stage.

posed by a selected optimization algorithm (including Evolutionary Algorithms, Game Strategies, Gradient-based Methodologies, Response Surfaces, Adaptive and Automatic methodologies), up to the specified objectives are satisfied. In this modular environment, each component of the optimization process, including input variables, input files, scripts or direct interfaces to run the software, output files, output variables and objectives, is defined as a node to be connected with the other components [13]. The complete logic flow from parameterization to performance evaluation is defined by the user who can select among several available optimization algorithms, according to the defined objectives. Statistical and visualization tools, can then be used for an efficient decision making, allowing the designer to select the optimal configuration of the system [14] [15].

The workflow implemented for the optimization of the A-Class foils followed the scheme reported in Figure 9 in appendix. The starting reference geometry is updated each cycle, by the morphing procedure described above, according to the design variables selected by the decision making criterion. The candidate evaluation process is managed by a script procedure written in *Scheme* language. The analyses at the two sailing conditions are performed in sequence. The upwind analysis is run if the downwind analysis was successful.

The downwind analysis begins at the maximum sinkage (hull flying around 15 cm from the water surface). If the lift generated is higher than target, the computation progresses trimming the sinkage up to the vertical equilibrium, otherwise the design is rejected. In upwind conditions, as stated, three computations are run to select the leeway angle that generates the required side force. If the final solution do not lay in the linear aerodynamic polar region, the candidate is rejected.

A two-objectives optimization was performed adopting the MOGA-II, a proprietary version of the Multi-Objective Genetic Algorithm [16]. The two defined objective functions were the minimization of the total drag at the two sailing conditions. The evaluation of the hull drag fraction in upwind condition was included in the *modeFRONTIER* environment by a node that, after the foils CFD analyses, executes the analytical hull drag model developed in form of a *Scilab* function.

## 5 Solutions

The time elapsed to complete the evaluation of one valid design, using the coarse mesh, ranged between 15 and 20 minutes on a workstation equipped with 20 CPU (2 processors Intel Xeon E5-2680 2.8 GHz with 10 cores each). The time required for the morphing action was less than two minutes. More than 400 evaluations were performed in three days. Among them about 40% of design candidates were rejected because of failure in the minimum lift requirement criterion. The solution obtained is reported in Figure 8.

The green point on the Pareto front is the optimum solution which is considered the best compromising design. The red circle refers to the starting baseline geome-

try which was built roughly referring to existing designs. The estimated drag reduction in upwind sailing is 7% (hull plus foils) while in downwind is 7.9%.

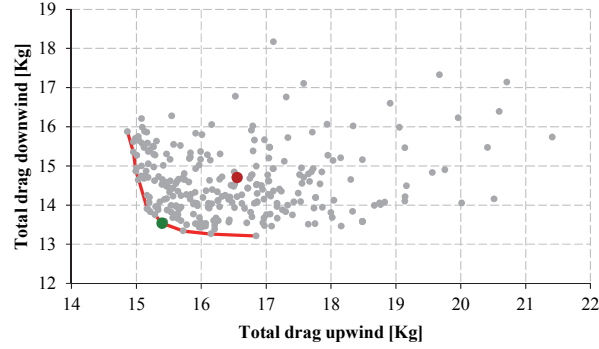


Figure 8: Pareto solution of the final two-objectives optimization

### 5.1 Post design verification

The selected optimum was verified in downwind conditions (only) using the fine mesh adopted for the grid sensitivity evaluation. The RBF solutions were applied to the fine baseline grid (the method is meshless) to obtain the fine mesh of the optimum geometry. The analysis also allowed to verify if the evaluation of the improvement is confirmed. The results of this verification is summarized in Table 1. The improvement was overestimated by only 0.24% confirming the coarse grid, despite the lower absolute accuracy it involves, to be suitable to correctly drive the optimization process toward the optimum.

Table 1: Drag solutions in downwind conditions.

<i>Mesh</i>	<b>Baseline</b>	<b>Optimized</b>	<i>Drag reduction</i>
	<i>Kg</i>	<i>Kg</i>	<i>%</i>
Coarse	14.7	13.54	7.89
Fine	13.99	12.92	7.65

## 6 Conclusions

A design procedure, based on multi-objective optimization, has been presented. The core of the method is the parameterization of the geometry implemented by a mesh morphing technique based on Radial Basis Functions. A pilot study has been setup to prove the capability of the RBF parametrization approach to face complex and strongly constrained design problems. The foils of an A-Class catamaran have been optimized at two sailing conditions. A multi-objective optimization, using

genetic algorithms, was setup within the *modeFRONTIER* environment. The analysis of candidates was implemented by a script procedure used to:

- drive the morphing of the numerical domain, according to the variables of design, by the *RBF Morph* tool;
- run in sequence the computations at the two sailing conditions trimming the attitudes to generate the required side force (in upwind sailing conditions) and vertical lift component (in downwind sailing);
- extract the information required to compute the objective functions.

The script is executed within the *ANSYS Fluent* CFD solver. The target of design was the minimization of drag in the two operating conditions. During upwind sailing, the boat is not supposed to fly. The total drag was, in this condition, integrated adding the drag component of the hull estimated by an analytical model (rudders are excluded) and integrated in the process by a node in *modeFRONTIER* that execute a function in the *Scilab* environment.

The optimization process led to a Pareto front on which a compromising design, that improved the performance by 7% in upwind conditions and by 7.9% in downwind, has been selected. Since the main objective of the work was to demonstrate the efficiency of the proposed approach to design, a very light mesh (less than one millions of hexahedral cells) was used in the optimization workflow. It was observed, however, a difference in the estimation of improvement, comparing the percentages of improvement computed using the coarse and a very fine grid, of only 0.24%, indicating the adoption of a so coarse mesh to provide a very efficient compromise between computational costs and optimization trend evaluation.

The work demonstrated the RBF mesh morphing approach to be a very good option to face complex constrained parametrization problems. It does not require to define a parametric CAD model and offers several advantages: no re-mesh required, high robustness, high parallelizability, meshless properties. The possibility to combine several RBF solutions and to define each amplification factor according to any formulation able to account for external constraints offer large flexibility in setting up complex parameterizations. The high parallelizable feature, furthermore, extend the potentialities of the method by providing the possibility, within HPC environments, to setup optimization configurations that involve large computational domains.

## References

- [1] Matthew Sheahan, “*High-speed sailing*”, *Ingenia*, Royal Academy of Engineering, Issue 57, December 2013.
- [2] Stefan Jakobsson and Olivier Amoignon, “*Mesh deformation using radial basis functions for gradient-based aerodynamic shape optimization*”, *Computers & Fluids*, 36(6), pp 1119-1136, July 2007.

- [3] M.E. Biancolini et al., “*Industrial application of the meshless morpher RBF morph to a motorbike windshield optimisation*”, In 4<sup>th</sup> European Automotive Simulation Conference, Munich, Germany, 6-7 July 2009.
- [4] Ubaldo Cella, Corrado Groth, and Marco E. Biancolini, “*Geometric Parameterization Strategies for shape Optimization Using RBF Mesh Morphing*”, in Advances on Mechanics, Design Engineering and Manufacturing, pp 537-545, September 2016.
- [5] Viola I. M., Biancolini M. E., Sacher M., Cella U., “*A CFD-Based Wing Sail Optimization Method Coupled to a VPP*”, 5<sup>th</sup> High Performance Yacht Design international conference, 8-12 March 2015, Auckland (NZ).
- [6] Marco E. Biancolini, “*RBF morph mesh morphing ACT extension for ANSYS Mechanical*”, In Automotive SimulationWorld Congress, Tokyo, Oct. 2014.
- [7] Larsson L. and Eliansson R. E., “*Principle of Sailing Yacht Design*”, Adlard Coles Nautical, London, UK, 1997.
- [8] Claughton, A.R., Sheno, R., Wellicome, J.F., “*Sailing Yacht Design: Theory*”, Addison Wesley, Longman, 1998.
- [9] Michele Stroligo, “*Preliminary Design Investigation for the development of new hull shapes for America’s Cup Class catamaran AC-62*”, International CAE Conference 2015, Verona, Italy, 19-20 October 2015.
- [10] Sighard F. Hoerner, “*Fluid-Dynamic Drag*”, Hoerner Fluid Dynamics, Bakersfield, CA (US), 1965.
- [11] Ubaldo Cella, Francesco Salvatore, Raffaele Ponzini, “*Coupled Sail and Appendage Design Method for Multihulls Based on Numerical Optimisation*”, PRACE – EU SHAPE Project final report, 5<sup>th</sup> July 2016.
- [12] David A. Caughey, “*Introduction to Aircraft Stability and Control*”, Course Notes for M&AE 5070, Cornell University, New York 14853-7501, 2011.
- [13] G. Vernengo, “*Design by Optimization of Ship Hull Forms. New perspectives through full parametric modelling and multi-objective optimization*”, modeFRONTIER International Users Meeting, 2014, Italy.
- [14] Clarich A. et al., “*Ottimizzazione della regolazione di una vela rigida per catamarani da regata mediante modeFRONTIER e ANSYS*”, ANSYS User Group Meeting. Italy, June 2013.
- [15] M. Bonci, M. Viviani, R. Broglia, G. Dubbioso, “*Method for estimating parameters of practical ship manoeuvring models based on the combination of RANSE computations and System Identification*”, in Applied Ocean Research, Volume 52, August 2015, pp 274-294.
- [16] D. Quagliarella, J. Périaux, C. Poloni, and G. Winter, “*Genetic Algorithms and Evolution Strategies in Engineering and Computer Science*”, Recent Advances and Industrial Applications, pp. 267-288, John Wiley & Sons.

## Appendix

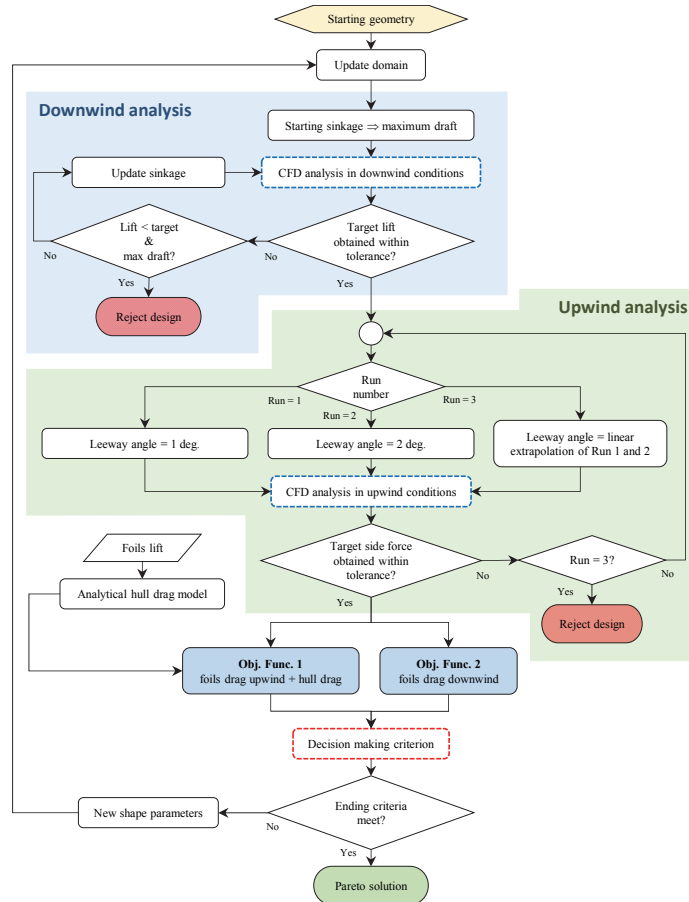


Figure 9: Flowchart of the optimization procedure.

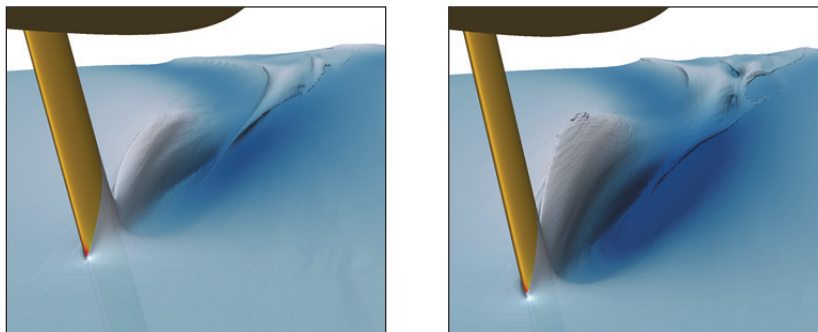


Figure 10: Free surface in downwind sailing by baseline (left) and optimum (right).